Hindawi
Advances in Materials Science and Engineering
Volume 2018, Article ID 6386280, 10 pages
https://doi.org/10.1155/2018/6386280

Research Article

Evaluation of Self-Healing Performance of PE and PVA Concrete Using Flexural Test

Choonghyun Kang,[1] Jungwon Huh ,[1] Quang Huy Tran ,[1] and Kiseok Kwak[2]

[1]*Chonnam National University, Yeosu, Republic of Korea*
[2]*Geotechnical Engineering Research Institute, KICT, Goyang, Republic of Korea*

Correspondence should be addressed to Jungwon Huh; jwonhuh@chonnam.ac.kr

Received 19 January 2018; Accepted 26 March 2018; Published 14 May 2018

Academic Editor: Julian Wang

The self-healing performance of PE and PVA concrete was evaluated, by using the three-point bending test with a notch. Four different crack inducement days were applied (7, 28, 49, and 91 days), and the same 21 days of healing period were applied to each case. The self-healing environments were in 20°C water, and in the curing room with 20°C temperature and 60% humidity. The flexural strength and the initial flexural stiffness of before and after healing were compared. As a result, both the strength recovery effect and the stiffness recovery effect decreased with the delay of crack inducement, and specimens in the water environment showed higher healing effect than those in the air environment. PVA fiber showed a relatively greater recovery effect than PE fiber.

1. Introduction

Self-healing of concrete is focused on a good solution to not only decrease the lifecycle cost but also to ease an environmental problem. Previous studies have mainly focused on improving the strength and durability of concrete. As a result, ultrahigh-performance concrete of over 150 MPa was developed, and concrete of 30 MPa is applied in the field [1–4]. The use of additives (such as fly ash) is also applied, to increase the durability of concrete [5–7]. The main focus of these studies is to reduce the construction cost, by reducing the cross section of the structure members. Meanwhile, other studies reported that the total cost maintenance of concrete structure for 30 years is similar to that of the construction cost [8–10]. The self-healing method is attracting attention in relation to maintenance cost reduction. The self-healing method causes the concrete structure to recover by detecting a deterioration itself and making possible an appropriate response before serious damage is developed. An appropriate response means timely correct repair or reinforcement, resulting in reduced maintenance cost [11, 12]. In addition, the increase in the overall service life of concrete structures will reduce the generation of carbon dioxide from cement production, positively affecting the environment in the long run.

Self-healing of concrete has been studied from various aspects over the past decade. The most well-known research is on a capsule containing an adhesive agent [13, 14]. The capsule is located at the crack propagation break, and the adhesive agent flows and recovers the crack automatically. A bacterium, which is an organic material, was investigated [15, 16]. It helps or maximizes the production of substances favorable for self-healing. These techniques can be categorized as an active method because they actively prepare cracks during the design and construction sequence, and the JCI self-healing committee defines this as Activated Repairing. On the other hand, passive self-healing is classified into Natural Healing, which is the recoverability of the concrete itself, and Autonomic Healing, which improves the self-healing performance of additional materials. Natural Healing and Autonomic Healing are classified as Autogenous Healing. However, Autonomic Healing can be classified as an active method because of the use of additional materials. Autonomic Healing and Activated Repairing are

Table 1: Mix proportion of fiber concrete.

Fiber	W/C (%)	s/a (%)	Volume fractions of fiber (%)	Unit content (kg/m^3)						Additive (cc/m^3)
				Water	Cement	Sand	Gravel	Fly ash	Fiber	SP
PE PVA	45	47	0.25 0.19	175	389	618	879	137	2.43	0.97

SP, superplasticizer.

Table 2: Properties of cement and aggregates.

Component	Density (g/cm^3)	Absorption (%)
Portland cement	3.15	—
Gravel	2.58	0.2
Sand	2.51	3.2

Table 3: Properties of fly ash.

SiO_2	53.98%
Moisture	0.01%
Loss on ignition	1.00%
Density	2.27 g/cm^3
Specific surface area	3,460 cm^2/g
Activity index	85% (28 days) 100% (91 days)

classified as Engineered Healing/Repairing. In a large category, all of them are designated as self-healing/repairing [17]. In recent years, self-healing has been studied not only in ordinary concrete but also in modified composites such as ECC [18].

The purpose of this study was to investigate the self-healing performance of concrete containing fly ash and fiber for improving healing performance. One important aspect of self-healing research is how to measure it, and various techniques have been tried in the past studies. This study selected the bending test in which the direct measurement of self-healing using the same specimen is possible. The self-healing performance was evaluated by comparing the flexural load and the flexural stiffness before and after the crack, using the notched specimen.

2. Experiment

2.1. Materials and Mixes. Table 1 shows the mix proportion of the two kinds of concrete prepared in this study. Depending on the fiber type, two proportions were determined, and the type and amount of the other materials were the same. Ordinary Portland cement, river gravel, and standard sand were used. Table 2 shows the properties of cement and aggregates estimated at preliminary experiments. Fly ash, which is reported to improve the durability of concrete, is also reported to help recovery by the precipitation of calcium carbonate ($CaCO_3$) and pozzolanic reaction [19, 20]. This study used fly ash with silicon dioxide (SiO_2) content of over 50%, and Table 3 shows the detailed physical properties. Fly ash was added of 50% of the cement volume. The water-cement ratio (w/c) was 45%, and the water-binder ratio (w/b) was 33.3%. Sand-to-aggregate (s/a) ratio was 47%. The air-entraining (AE) water-reducing agent was added to improve the workability. It has been reported that the polypropylene fiber embedded in concrete acts as a bridge between the crack surfaces and affects precipitation during the healing period. This study prepared polyethylene (PE) fiber and polyvinyl alcohol (PVA) fiber. Figure 1 shows the samples of each fiber, and Table 4 shows the properties of the fibers. As far as possible, different properties were applied equally in order to compare only differences according to fiber types. However, it is difficult to perfectly match the two fiber concretes since the thickness and density of the fibers are different, so the same weight was applied for the convenience of an experiment.

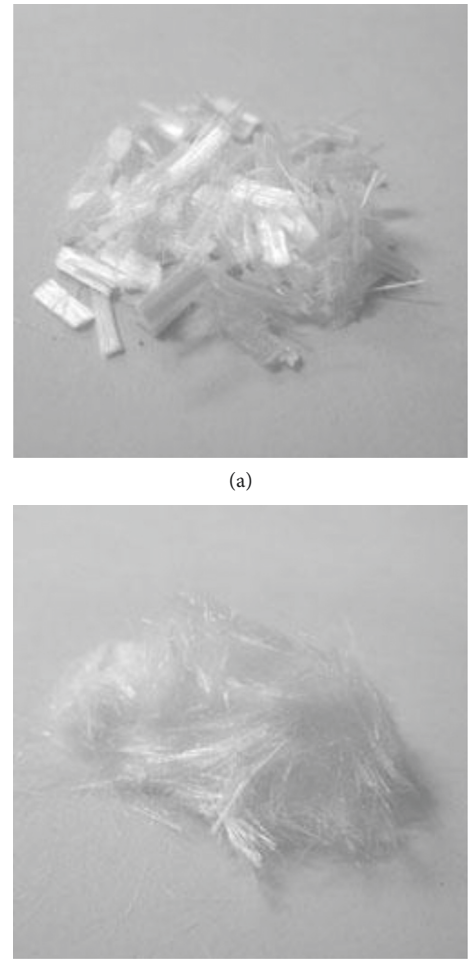

(a)

(b)

Figure 1: Sample of fibers: (a) polyethylene fiber; (b) polyvinyl alcohol fiber.

2.2. Specimen. Prismatic specimens of L400 mm × W100 mm × D100 mm with a notch were prepared in this study. Figure 2 shows the dimension and the experimental view. Since concrete is a brittle material, cracks develop rapidly. Since concrete

Table 4: Properties of fibers.

Content	PE	PVA
Length	4 mm	4 mm
Diameter	0.012 mm	0.040 mm
Density	0.97 g/cm^3	1.30 g/cm^3
Elastic modulus	88 GPa	41 GPa
Tensile strength	2,700 MPa	1,560 MPa

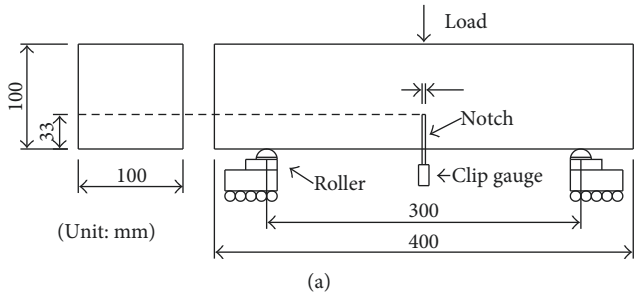

(a)

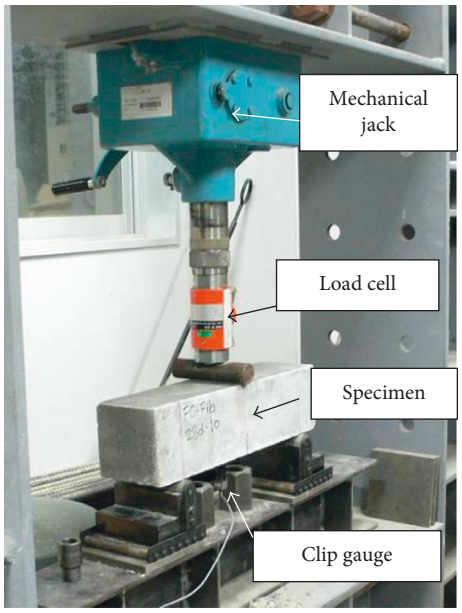

(b)

Figure 2: Flexural test: (a) specimen size; (b) test view.

is a nonhomogeneous material, it is difficult to specify the location of the cracks. This is why the notch was applied in this study. The depth of the notch determines the maximum flexural load, and RILEM recommends a notch of 20–25% of the specimen thickness [21]. However, it has been confirmed through preliminary experiments that it is difficult to control crack propagation, because the propagation speed of the cracks is too fast, due to the high maximum flexural load. In the case of a notch being too deep, it was judged that the crack generation region where self-healing will be performed is too narrow to allow evaluation of the self-healing performance. We concluded that the application of 33 mm, which is 1/3 of the specimen thickness, is effective for both crack control and evaluating the self-healing performance. The introduction of the notch can be classified into a preintroduction method, in which an acrylic bar or the like is installed and removed, and a postintroduction method, in which a cutter is used. The latter has some problems, in that it can introduce some damage to the specimen during cutting, but it is easier than the former. No significant difference was found in the posthealing behavior of the mutual comparisons through preliminary experiments. The posthealing behavior depends on the crack depth that could be healed by self-healing, and this is formed almost constant during the loading sequence. The notch introduction was conducted at 7 days after casting, which is the fastest loading day of all cases, and a diamond wet cutter was used.

Table 5: Cases and test program.

Case	Days after casting		Healing	
	1st and 2nd loading	3rd loading	Condition	Period
PE-7–28-A PVA-7–28-A PE-7–28-W PVA-7–28-W	7	28	Air Water	21 days
PE-28–49-A PVA-28–49-A PE-28–49-W PVA-28–49-W	28	49	Air Water	21 days
PE-49–70-A PVA-49–70-A PE-49–70-W PVA-49–70-W	49	70	Air Water	21 days
PE-91–112-A PVA-91–112-A PE-91–112-W PVA-91–112-W	91	112	Air Water	21 days

Each specimen was cast in a steel prismatic mold after mixing. Then, 24 hours later, specimens were demolded and cured in fresh water with a temperature of (20 ± 3)°C. Crack inducements (1st loading) were conducted at 7, 28, 49, and 91 days from the casting. The 2nd loading was conducted just after crack inducement, and it was the control value before the self-healing. The same 21 days of the healing period were applied to specimens after the 2nd loading. The self-healing environment was different for each case, such as in water and air. The water environment means healing in fresh water with a temperature of (20 ± 3)°C, which is the same condition as the curing after casting. The air environment means healing in the curing room with a temperature of (20 ± 3)°C and relative humidity of 60%. The 3rd loading was conducted after the healing period, and it was the evaluation value of the self-healing performance. Table 5 shows the test program.

The case was named considering the fiber name, the crack induction (1st loading) and 2nd loading, the 3rd loading, and the self-healing environment. For example, PE-7–28-W means that the specimen is PE fiber concrete, the crack induction and 2nd loading were conducted at 7 days after casting, the 3rd loading was conducted at 28 days after casting, and specimens were cured in the water condition after crack inducement. All cases had four specimens.

2.3. Flexural Test. The most important process in the evaluation of the self-healing of concrete is to generate an adequate crack. Van Breugel reported that a crack with only

less than 0.2 mm width could be expected to recover by self-healing [22]. This study used a crack mouth opening displacement (CMOD) by measuring a clip gauge set at the notch opening, and CMOD controlled the crack width during loading. Meng et al. reported that the effects of the notch-to-depth ratio are associated with the loading rate, and it is less than 10% at a deflection rate up to 1.25 mm/min [23]. But the loading speed of this study was 0.5–1.0 mm/min; therefore, the effect is insignificant.

The self-healing performance was evaluated by three-times loading. The crack inducement (1st loading) was the process to make an adequate crack. The exact crack width could not be measured, but CMOD makes an almost constant crack width because the crack width and CMOD are linearly proportional [24]. The unloading point was set as CMOD 0.05 mm, which is a point after the peak load. After finishing the unloading of the crack inducement (1st loading), the 2nd loading was conducted. To prevent further crack propagation, the unloading point of the 2nd loading was the same as CMOD 0.05 mm. The next process was the healing. Specimens were healed in water and air, respectively, by case. Lastly, the 3rd loading was conducted. The 3rd loading was to evaluate the self-healing performance, and loading was performed, until the specimen was completely separated.

Figure 3 shows a typical load-CMOD curve. The peak load appeared between 0.02 and 0.03 mm CMOD, and the unloading point was the load-drop region. Both load and CMOD decrease during the unloading sequence, and a right downward convex curve was drawn. The 2nd loading curve was similar to the 1st loading curve, as a left upward convex curve, and the maximum load of the 2nd loading was lower than the peak load of the 1st loading. The unloading curve after the 2nd loading was also a right downward convex curve, and the unloading completion points after both the 1st loading and the 2nd loading were almost the same. The 3rd loading curves were different by case. According to the degree of self-healing, the curves were drawn near the curve of the 2nd loading, and the maximum load point also appeared at a different point, not CMOD 0.05 mm.

2.4. Evaluation of Self-Healing Performance

2.4.1. Flexural Strength. Firstly, the flexural strength of cases was compared. Granger et al. also used the flexural strength comparison for evaluation of the self-healing performance [25]. However, the flexural strength of the healed specimen was compared with the flexural strength of the unhealed specimen. Relative flexural strength recovery could be compared, but it is not a direct comparison because it is not a comparison of values from the same specimen. This study compared two values before and after self-healing from the same specimen. The reference point was CMOD 0.05 mm, and the comparison target was the maximum load value of the 3rd loading. The flexural behavior after deterioration generally decreases, compared to that before deterioration. This is the reason why the maximum load of the 2nd loading is lower than the load of the unloading point of the 1st loading, even though the CMOD was the same at 0.05 mm. If the maximum load of the 3rd loading is greater than the load of the unloading point of the 1st loading, the self-healing contributed to the strength recovery. In this study, the ratio between the maximum load of the 3rd loading and the load of the unloading point of the 1st loading is called the strength recovery effect. If the strength recovery effect is higher than 1.0, this means that the self-healing restored the flexural strength.

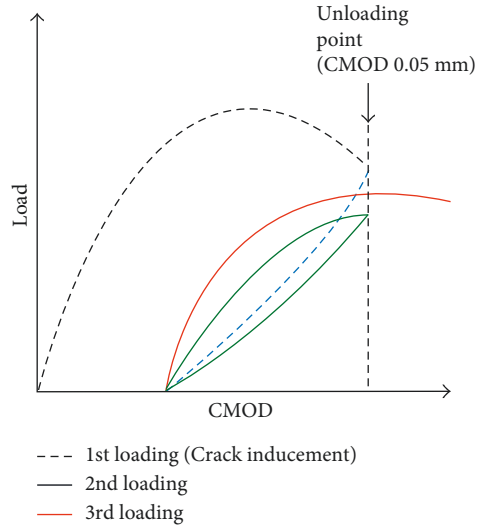

Figure 3: Typical load-CMOD curve.

2.4.2. Flexural Stiffness. Self-healing evaluation by flexural strength implies the aging effect of an uncracked part. After casting, concrete has a constant hydration reaction. The flexural strength means the maximum load carrying capacity of the whole section, such as cracked and uncracked parts. In other words, the aging effect of the uncracked part cannot be avoided. In order to accurately evaluate the self-healing performance, it is necessary to distinguish the recovery effect from the aging effect. However, it is not easy to separate the self-healing effect from the aging effect in the flexural strength comparison.

This study focused on the different initial behaviors of the load-CMOD curve of the 2nd and the 3rd loading. It is known that the load-CMOD gradient in the three-point bending test is proportional to the modulus of elasticity of the specimen [26, 27]. The initial behavior of the load-CMOD curve is related to the crack opening, so the change of the crack circumstance will be represented most sensitively. Figure 4 shows the initial behavior of the load-CMOD curve of the 2nd and the 3rd loading of PE-7–28-W and shows the different initial slopes by the loading. This study estimated the initial slope of the load-CMOD, which used data from the start point CMOD to (0.003–0.005) mm. The ratio between the initial slope of the 3rd loading and that of the 2nd loading is known as the stiffness recovery effect. If the stiffness recovery effect is higher than 1.0, this means that the self-healing restored the flexural stiffness.

3. Results and Discussion

3.1. Load-CMOD Curve. The load-CMOD curves of the 1st loading (crack inducement) and the 2nd loading were

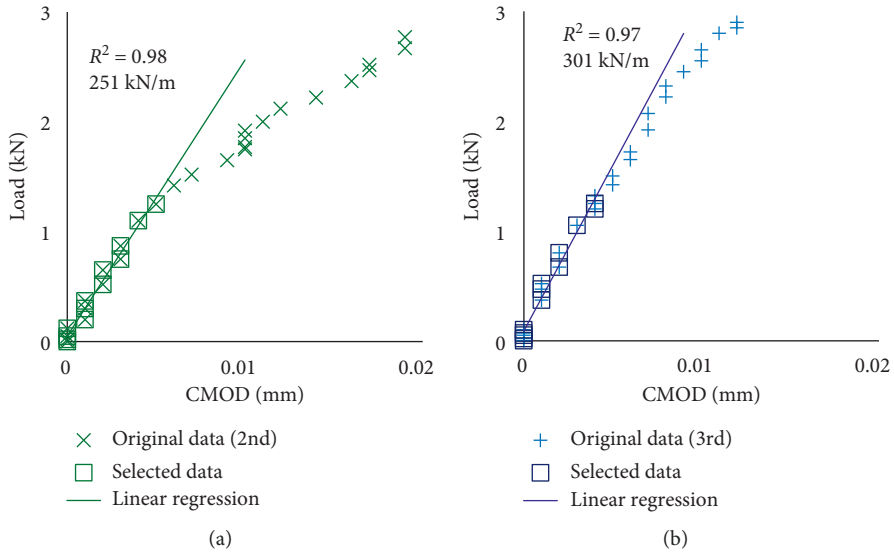

Figure 4: Example of the initial slope of the load-CMOD curve of (a) the 2nd loading and (b) the 3rd loading (PE-7–28-W).

similar, regardless of the variables. Figure 5 shows typical load-CMOD curves of PE concrete with different 1st loading days and different self-healing environments, respectively. Figure 6 shows typical load-CMOD curves of PVA concrete with different 1st loading days and different self-healing environments, respectively. The peak load appeared between CMOD 0.02 and 0.03 mm. The maximum loads of the 2nd loading were measured at CMOD 0.05 mm, and the peak load of the 3rd loading was measured. Tables 6 and 7 show the detailed load value of PE and PVA concrete, respectively. The peak load increased with a delay of the 1st loading days, and the average peak load increased as in Figure 7. The average peak loads of PVA concrete were higher than those of PE concrete (except the case of 49 days), but the difference was not significant, considering the deviation. A load of the unloading point increased with increase in the peak load and was about 87%. The CMODs of the unloading completion after the 1st loading were 0.016 ± 0.002 mm, and it was confirmed that there was no correlation between the type of fiber and the 1st loading days. This indicates that the degree of crack propagation was almost constant, regardless of the variables. The slopes of the load-CMOD curve of the 2nd loading were lower than those of the 3rd loading, but a certain pattern due to the specimen did not appear. The maximum load of the 2nd loading was $(95 \pm 3)\%$ of the load of the unloading point, regardless of the variables. The CMOD of the unloading completion after the 2nd loading was almost the same as that of the 1st loading.

The behavior of the load-CMOD curve of the 3rd loading after healing showed different patterns, depending on the 1st loading day and the self-healing environment. If the initial slope of the load-CMOD curve of the 3rd loading was greater than that of the 2nd loading, the maximum load of the 3rd loading was also greater than that of the 2nd loading. The CMOD at the maximum load also increased and was over 0.05 mm. In contrast, if the initial slope of the load-CMOD curve of the 3rd loading was smaller than that of the 2nd loading, the maximum load of the 3rd loading was also smaller than that of the 2nd loading. Except for the 7–28 and 28–49 cases, which have relatively fast 1st loading days, the maximum load was smaller than that of the 2nd loading.

3.2. Flexural Strength Recovery Effect. Figure 8 shows the flexural strength recovery effect with different 1st loading days and different self-healing environment of PE concrete and PVA concrete, respectively. Firstly, both the PE-7–28 case and PVA-7–28 case had the strength recovery effect of over 1.0, regardless of the self-healing environment. This means that the maximum load of the 3rd loading is greater than the load of the unloading point of the 1st loading. In other words, the flexural strength of the section was recovered during the healing period. At only 7 days after casting, the ratio of unhydrated cement in the specimen may be quite high, and it means that an aging can happen not only in the uncracked part but also in the cracked part. The strength recovery effect of over 1.0 in 7–28 cases could be explained as being due to this significant aging effect. However, the strength recovery effect decreased with the delay of the 1st loading day; in particular, the values of the PE concrete with air environment showed less than 0.5. This means that the specimen did not recover at all. The deterioration during the 2nd loading could be the reason for the decrease in flexural strength. The strength recovery effect with water environment decreased continuously with the delay of the 1st loading day, but it converged for the 91–112 cases.

In air environment, there was a prominent difference between the PE and PVA concrete. The strength recovery effect of the PE-28–49-A case shows a sharp fall, and after that, it is almost constant. On the other hand, the strength recovery effect of PVA concrete with air environment shows a gradual decrease pattern, and the PVA-7–28-A and PVA-28–49-A cases show similar values to the PVA-7–28-W and PVA-28–49-W cases. It is presumed that the hydrophilicity of PVA fiber has affected the strength recovery effect.

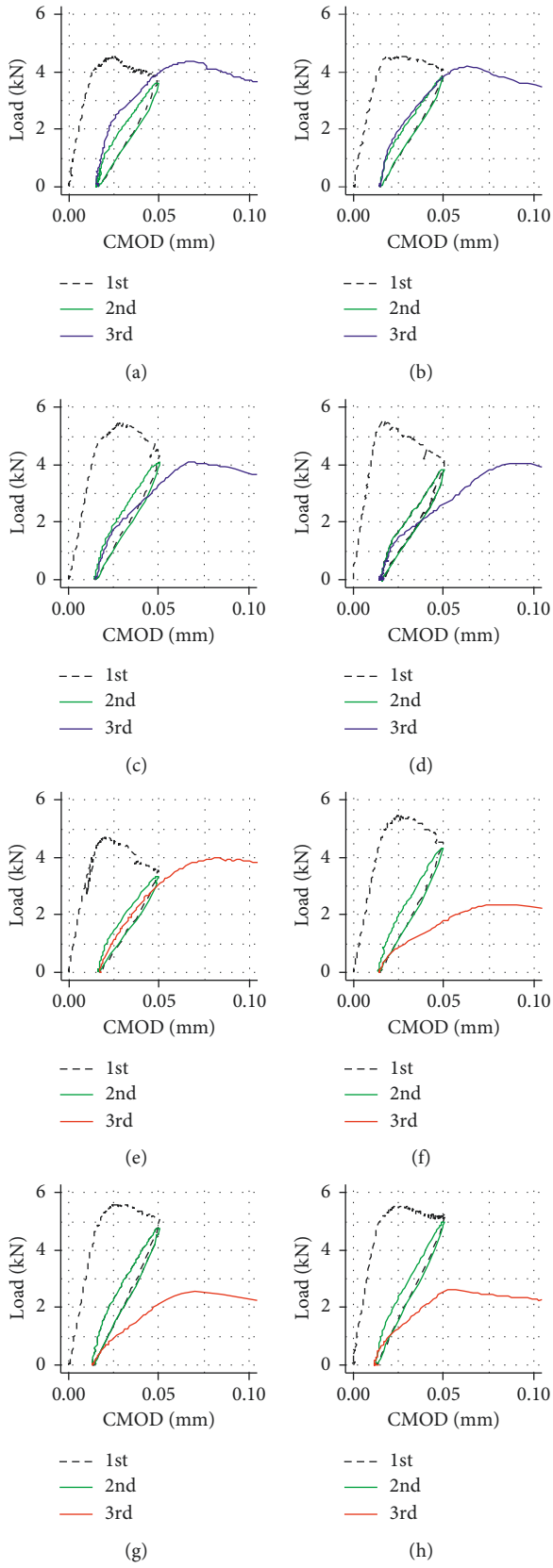

Figure 5: Typical load-CMOD curves of PE concrete: (a) PE-7–28W, (b) PE-28–49-W, (c) PE-49–70-W, (d) PE-91–112-W, (e) PE-7–28-A, (f) PE-28–49-A, (g) PE-49–70-A, and (h) PE-91–112-A.

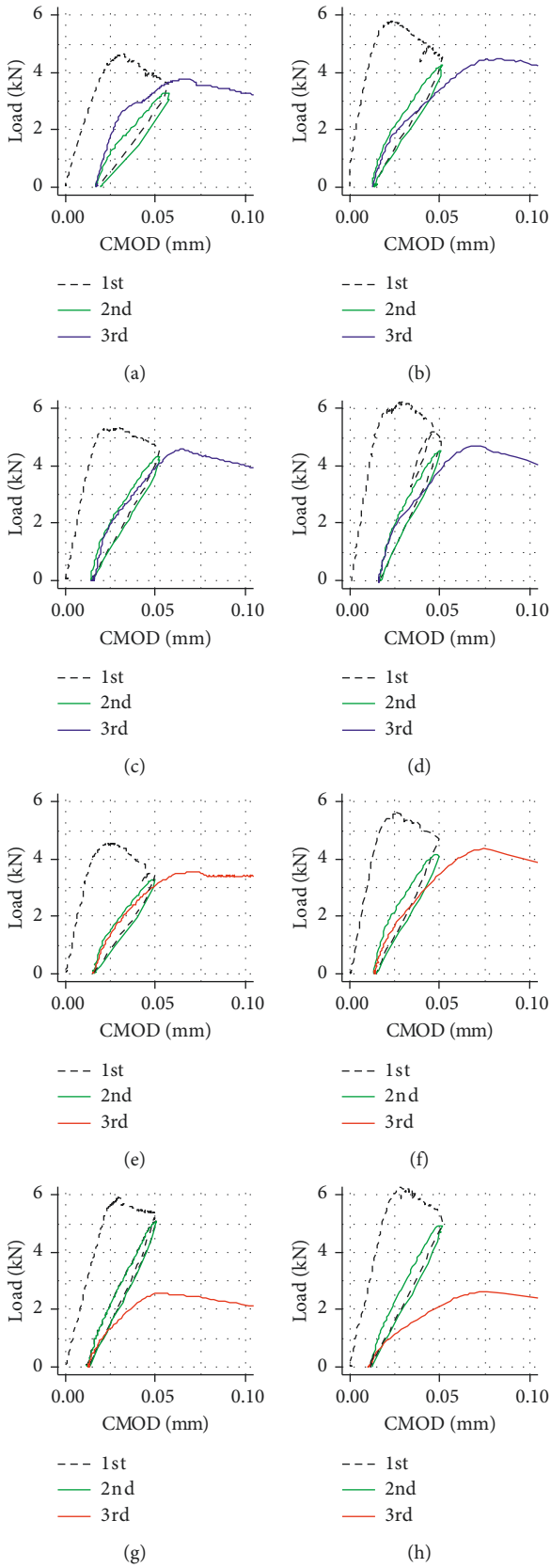

Figure 6: Typical load-CMOD curves of PVA concrete: (a) PVA-7–28W, (b) PVA-28–49-W, (c) PVA-49–70-W, (d) PVA-91–112-W, (e) PVA-7–28-A, (f) PVA-28–49-A, (g) PVA-49–70-A, and (h) PVA-91–112-A.

Table 6: Peak and maximum load of PE concrete.

Case	Peak/maximum load		
	1st loading	2nd loading (CMOD 0.05 mm)	3rd loading
PE-7–28-W	4.48	3.40	3.90
	4.53	3.83	4.38
	4.43	3.88	4.55
	4.60	3.75	4.30
PE-28–49-W	5.93	5.43	5.10
	4.58	3.95	4.20
	4.83	4.25	4.30
	5.30	4.43	4.55
PE-49–70-W	5.25	4.75	4.58
	5.98	5.20	4.95
	5.45	4.30	4.10
	6.15	5.48	5.13
PE-91–112-W	6.13	4.53	4.33
	6.48	4.70	4.58
	5.53	4.00	4.05
	5.48	4.85	4.88
PE-7–28-A	4.70	3.50	4.00
	4.78	3.45	4.08
	4.03	2.80	3.15
	4.50	3.55	4.63
PE-28–49-A	5.38	5.03	2.61
	5.65	4.85	2.45
	5.23	5.00	2.69
	5.45	4.53	2.36
PE-49–70-A	5.60	5.08	2.55
	5.60	5.10	2.59
	5.50	5.18	2.56
	6.30	5.30	2.46
PE-91–112-A	5.53	5.23	2.64
	5.73	3.95	2.04
	5.88	3.95	2.18
	4.95	4.50	2.04

Table 7: Peak and maximum load of PVA concrete.

Case	Peak/maximum load		
	1st loading	2nd loading (CMOD 0.05 mm)	3rd loading
PVA-7–28-W	4.40	3.23	3.60
	4.85	3.88	4.05
	4.63	3.63	3.78
	4.55	3.68	4.10
PVA-28–49-W	5.73	4.70	4.40
	5.55	5.55	5.53
	5.78	4.53	4.50
	6.15	5.38	5.03
PVA-49–70-W	5.35	4.65	4.28
	5.63	4.53	2.85
	5.35	5.00	5.08
	5.23	5.18	4.10
PVA-91–112-W	6.25	4.88	4.70
	6.10	5.60	4.50
	6.38	5.78	5.55
	6.83	6.63	4.90
PVA-7–28-A	4.55	3.45	3.55
	5.03	4.88	5.00
	4.50	4.20	4.53
	4.40	4.05	4.63
PVA-28–49-A	5.75	5.00	4.98
	5.65	4.68	4.35
	5.58	4.18	4.00
	5.38	4.50	4.12
PVA-49–70-A	5.20	4.90	3.96
	5.38	2.98	3.15
	5.93	5.38	2.71
	5.75	4.78	2.26
PVA-91–112-A	6.30	5.43	2.63
	5.45	5.08	2.63
	6.93	5.35	2.66
	—	—	—

The decrease in the strength recovery effect in inverse proportion to the delay of the 1st loading day is similar to the decrease in the strength increase ratio according to the aging effect. The strength increase capacity of the uncracked part may be high in 7–28 cases, but it must be lower than before in the 49–70 and 91–112 cases. In other words, the high strength recovery effect of the early 1st loading was dominant in the aging effect of the uncracked part, and it almost disappeared after 49 days. However the self-healing prevented further decrease.

3.3. Flexural Stiffness Recovery Effect. Figure 9 shows the flexural stiffness recovery effect with different 1st loading days and different self-healing environment of PE concrete and PVA concrete, respectively. The flexural stiffness recovery effect was inversely proportional to the delay of the 1st loading, regardless of the fiber type. The flexural stiffness recovery effect was over or around 1.0 with the water environment. This means that the initial slope of the load-CMOD curve of the 3rd loading was greater than that of the 2nd loading, and the recovery at the crack tip could be expected. Otherwise, the flexural stiffness recovery effects with air environment were less than 1.0, regardless of the fiber type.

The average stiffness recovery effect of PVA concrete was 13% higher than that of PE concrete, 13% higher in the water environment, and 51% higher in the air environment. In particular, the average stiffness recovery effect of the PVA-7–28-W case shows over 1.4, and in the PVA-91–112-W case, over 1.0 was confirmed. These results are also attributed to the hydrophilicity of PVA fiber.

As a distinct difference between the air and the water environment of the stiffness recovery effect, the stiffness recovery effect more efficiently represents the self-healing performance. The reason is that the stiffness recovery effect was evaluated using the limited crack tip part where the healing effect was concentrated. It cannot be concluded that the stiffness recovery effect is the result of completely excluding the aging effect because it is also involved in not only the recovered crack tip part but also the enhanced uncracked part by the aging effect. Nevertheless, it can be deduced that the initial slope of the load-CMOD curve is influenced by the restoration of the flexural stiffness of the part where cracks are reopened, rather

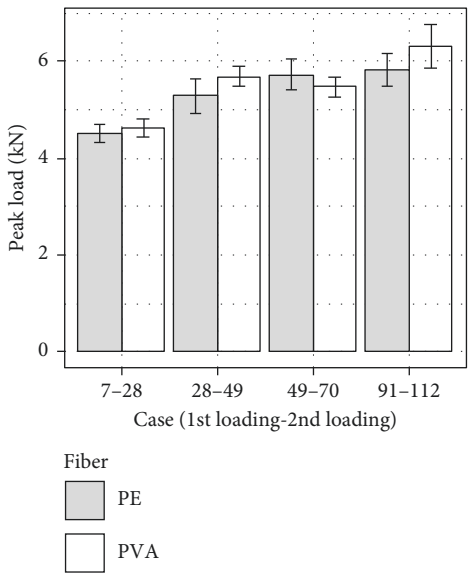

Figure 7: Peak load according to the 1st loading days.

than the aging effect. Therefore, it is considered to be an index that can more effectively evaluate the self-healing performance.

3.4. Crack Observation. Figure 10 shows the microscopic images of the 7–28 cases of PE and PVA concrete. It can be seen that debris-like substances are deposited all over the crack surface in the PE-W case, and the visual crack width appears to be relatively narrow. However, no precipitated material was observed around the fibers seen between the cracks. The PE-A case also showed deposited substances at the crack surface, but the amount was relatively small. The seen fiber between the cracks was also relatively clean. On the other hand, it was confirmed that not only the crack surfaces but also the bridged fiber had been covered by deposited substances in the PVA-W case. As mentioned above, it is considered as an additional evidence of why the PVA specimens showed a relatively high recovery in both strength and stiffness. The PVA-A case also showed deposited substances. However, the amount was relatively small, and the fibers appeared relatively clean.

This result does not represent the entire crack surface circumstance because the optical microscope can observe only a shallow depth from the surface. It was judged as a qualitative basis to supplement the quantitative comparison of the flexural strength and stiffness because almost similar patterns were observed in all the specimens tested in this study.

4. Conclusion

This study evaluates the self-healing performance with different crack inducement days and different self-healing environment. The PE concrete and PVA concrete were compared, and the flexural test using the notched three-point bending specimen was conducted. The results are summarized as follows:

(1) Regardless of the type of fiber, the degree of recovery of flexural strength and the flexural stiffness decreased in inverse proportion to the delay of the crack inducement day (1st loading). Moreover, the water environment always showed high recovery effect than the air environment in all cases. These results confirm that the fast crack inducement has an advantage for self-healing, and the water environment is more suitable for self-healing.

(2) The evaluated self-healing performance exhibits similar characteristics to the aging effect. The recovery effect decreases in inverse proportion to the crack inducement time, and it shows more recovery in the water environment. The self-healing performance is closely related to the aging effect, and this means that the self-healing performance contains a considerable aging effect.

(3) Comparison of the flexural strength before and after healing cannot completely exclude the aging effect because not only the cracked part, but also the

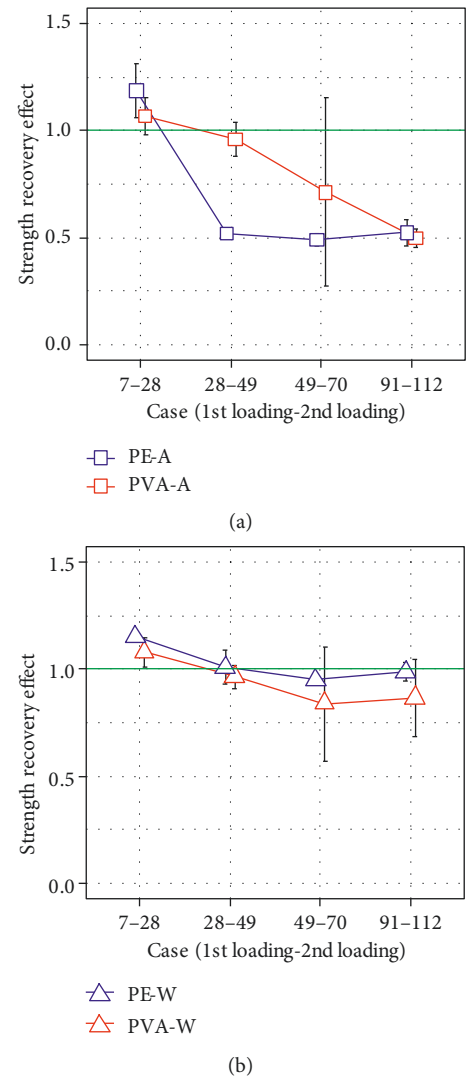

Figure 8: Strength recovery effect: (a) air environment; (b) water environment.

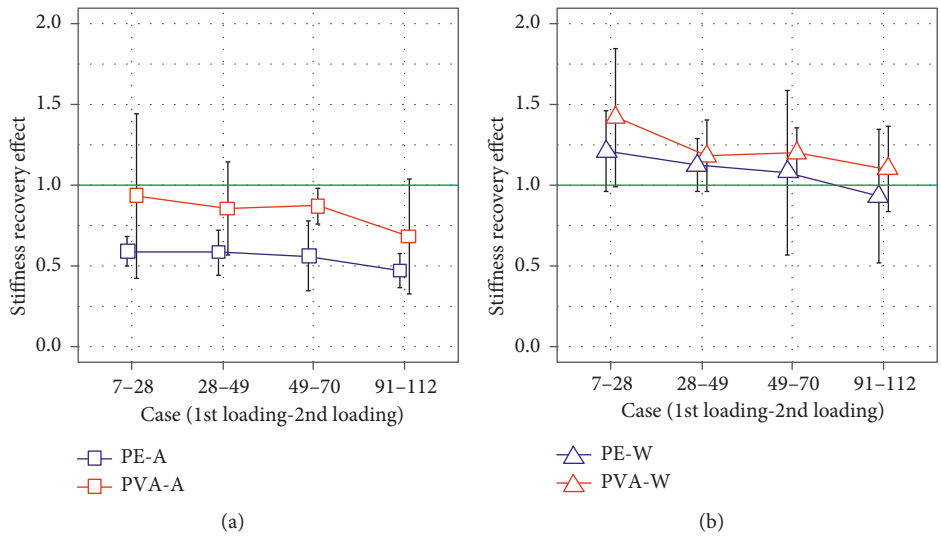

Figure 9: Stiffness recovery effect: (a) air environment; (b) water environment.

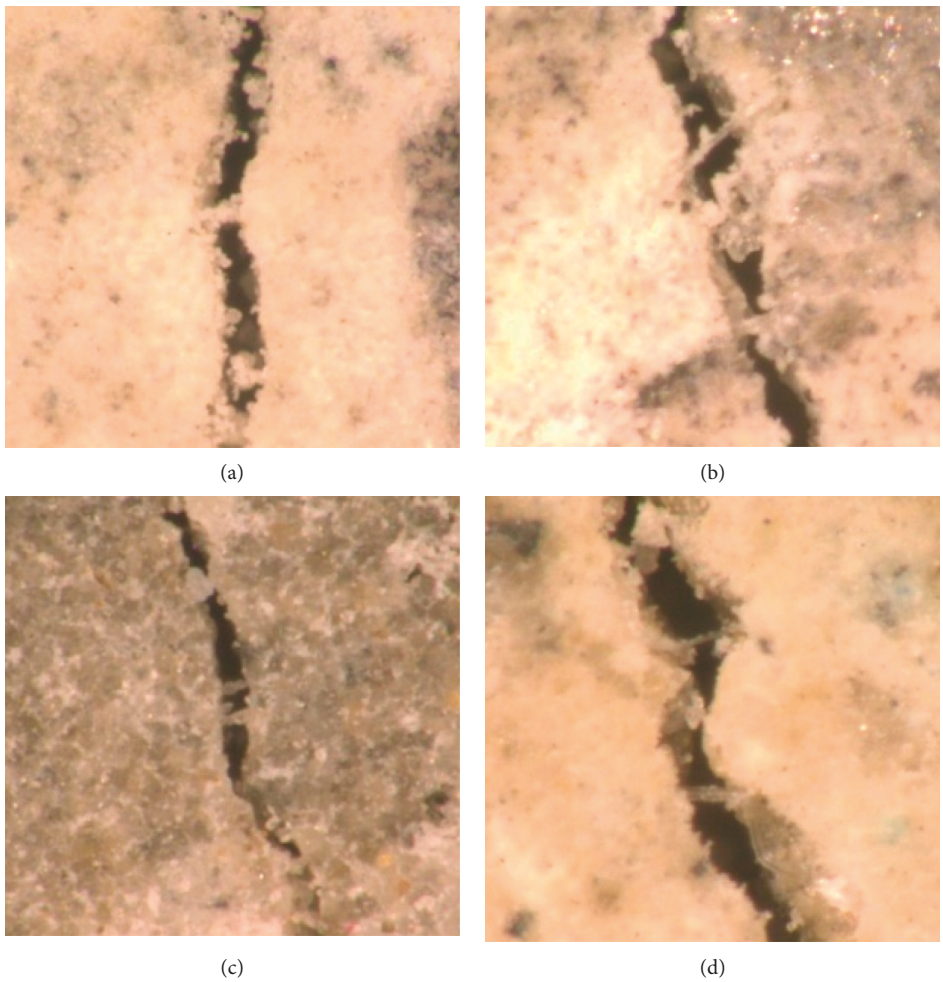

Figure 10: Optical microscopic images observed the crack surface: (a) PE-W, (b) PE-A, (c) PVA-W, and (d) PVA-A.

uncracked part participated in the strength. On the other hand, comparison of flexural stiffness is dominant at the crack tip, where the recovery due to self-healing is concentrated, and the aging effect is relatively small. It is considered that comparing the flexural stiffness, rather than the flexural strength, is

more appropriate for more accurate evaluation of the self-healing performance.

(4) PVA concrete has a relatively greater self-healing performance than PE concrete in both the air and water environment. It is considered that the hydrophilicity of PVA fiber has an effect.

Data Availability

The data used to support the findings of this study are available from the corresponding author upon request.

Conflicts of Interest

The authors declare that they have no conflicts of interest.

Acknowledgments

This research was supported by the Basic Science Research Program through the National Research Foundation of Korea (NRF) funded by the Ministry of Education (NRF-2017R1D1A1B03034470).

References

[1] G. A. Barbos and M. Pastrav, "State-of-the-art report on ultra-high performance concrete (UHPC)," *Constructii*, vol. 15, no. 1, pp. 63–69, 2014.

[2] A. Alsalman, C. N. Dang, G. S. Prinz, and W. Micah Hale, "Evaluation of modulus of elasticity of ultra-high performance concrete," *Construction and Building Materials*, vol. 153, pp. 918–928, 2017.

[3] W. Meng and K. Khayat, "Effects of saturated lightweight sand content on key characteristics of ultra-high-performance concrete," *Cement and Concrete Research*, vol. 101, pp. 46–54, 2017.

[4] Y. Bao, M. Valipour, W. Meng, K. H. Khayat, and G. Chen, "Distributed fiber optic sensor-enhanced detection and prediction of shrinkage-induced delamination of ultra-high-performance concrete overlay," *Smart Materials and Structures*, vol. 26, no. 8, p. 085009, 2017.

[5] A. Bilodeau and V. M. Malhotra, "High-volume fly ash system: concrete solution for sustainable development," *ACI Materials Journal*, vol. 97, no. 1, pp. 41–48, 2000.

[6] S. Cheng, Z. Shui, T. Sun, R. Yu, G. Zhang, and S. Ding, "Effects of fly ash, blast furnace slag and metakaolin on mechanical properties and durability of coral sand concrete," *Applied Clay Science*, vol. 141, pp. 111–117, 2017.

[7] H. Liu, Q. Zhang, V. Li, H. Su, and C. Gu, "Durability study on engineered cementitious composites (ECC) under sulfate and chloride environment," *Construction and Building Materials*, vol. 133, pp. 171–181, 2017.

[8] D. M. Frangopol, K. Y. Lin, and A. C. Estes, "Life-cycle cost design of deteriorating structures," *Journal of Structural Engineering*, vol. 123, no. 10, pp. 1390–1401, 1997.

[9] D. M. Frangopol and M. Liu, "Maintenance and management of civil infrastructure based on condition, safety, optimization, and life-cycle cost," *Structure and Infrastructure Engineering*, vol. 3, no. 1, pp. 29–41, 2007.

[10] V. W. Tam, S. Senaratne, K. N. Le, L. Y. Shen, J. Perica, and I. C. S. Illankoon, "Life-cycle cost analysis of green-building implementation using timber applications," *Journal of Cleaner Production*, vol. 147, pp. 458–469, 2017.

[11] S. J. Park and S. Y. Ghim, "Applications and prospects of calcium carbonate forming bacteria in construction materials," *Journal of Microbiology and Biotechnology*, vol. 40, no. 3, pp. 169–179, 2012.

[12] E. J. Choi, J. Wang, J. H. Yoon, S. E. Shim, J. H. Yun, and I. Kim, "Self-healing Engineering Materials: I. Organic materials," *Clean Techology*, vol. 17, no. 1, pp. 1–12, 2011.

[13] S. R. White, N. R. Sottos, P. H. Geubelle, and J. S. Moore, "Autonomic healing of polymer composites," *Nature*, vol. 409, no. 6822, pp. 794–797, 2001.

[14] E. N. Brown, S. R. White, and N. R. Sottos, "Microcapsule induced toughening in a self-healing polymer composite," *Journal of Materials Science*, vol. 39, no. 5, pp. 1703–1710, 2004.

[15] W. J. Kim, S. T. Kim, S. J. Park, S. Y. Ghim, and W. Y. Chun, "A study on the development of self-healing smart concrete using microbial biomineralization," *Journal of the Korean Concrete Institute*, vol. 21, no. 4, pp. 501–511, 2009.

[16] S. Qian, J. Zhou, and D. Rooij, "Self-healing behavior of strain hardening cementitious composites incorporating local waste materials," *Cement and Concrete Composites*, vol. 31, no. 9, pp. 613–621, 2009.

[17] S. Igarashi, M. Kunieda, and T. Hishiwaki, "Research activity of JCI technical committee TC-075B: autogenous healing in cementitious materials," in *Proceedings of 4th International Conference on Construction Materials: Performance, Innovations and Structural Implications*, pp. 89–96, Nagoya, Japan, August 2009.

[18] H. Liu, Q. Zhang, C. Gu, H. Su, and V. Li, "Self-healing of microcracks in Engineered Cementitious Composites under sulfate and chloride environment," *Construction and Building Materials*, vol. 153, pp. 948–956, 2017.

[19] P. Termkhajornkit, T. Nawa, and K. Kurumisawa, "Effect of water curing conditions on the hydration degree and compressive strengths of fly ash–cement paste," *Cement and Concrete Composites*, vol. 28, no. 9, pp. 781–789, 2006.

[20] R. H. Haddad and M. A. Bsoul, *Self-Healing of Polypropylene Fiber Reinforced Concrete: Pozzolan Effect*, Ph.D. dissertation, Jordan University of Science and Technology, Irbid, Jordan, 1999.

[21] TC162-TDF RILEM, "Test and design methods for steel fibre reinforced concrete: bending test," *Materials and Structures*, vol. 33, pp. 3–5, 2000.

[22] K. Van Breugel, "Self-healing en vloeistofdichtheid," *Cement*, vol. 7, pp. 85–89, 2003.

[23] W. Meng, Y. Yao, B. Mobasher, and K. H. Khayat, "Effects of loading rate and notch-to-depth ratio of notched beams on flexural performance of ultra-high-performance concrete," *Cement and Concrete Composites*, vol. 83, pp. 349–359, 2017.

[24] P.-E. Petersson, *Crack Growth and Development of Fracture Zones in Plain Concrete and Similar Materials*, Ph.D. dissertation, Lund University, Lund, Sweden, 1981.

[25] S. Granger, A. Loukili, G. Pijaudier-Cabot, and G. Chanvillard, "Mechanical characterization of the self-healing effect of cracks in Ultra High Performance Concrete (UHPC)," in *Proceedings Third International Conference on Construction Materials, Performance, Innovations and Structural Implications, ConMat*, vol. 5, pp. 22–24, Vancouver, Canada, August 2005.

[26] Y. Jenq and S. P. Shah, "Two parameter fracture model for concrete," *Journal of Engineering Mechanics*, vol. 111, no. 10, pp. 1227–1241, 1985.

[27] S. P. Shah, "Determination of fracture parameters (KIcs and CTODc) of plain concrete using three-point bend tests," *Materials and Structures*, vol. 23, no. 6, pp. 457–460, 1990.